

A comparison of the ideal strength between $L1_2\text{Co}_3(\text{Al}, \text{W})$ and Ni_3Al under tension and shear from first-principles calculations

Yun-Jiang Wang^{1,a)} and Chong-Yu Wang^{1,2}

¹Department of Physics, Tsinghua University, Beijing 100084, People's Republic of China

²The International Center for Materials Physics, Chinese Academy of Sciences, Shenyang 110016, People's Republic of China

(Received 21 March 2009; accepted 11 June 2009; published online 2 July 2009)

The ideal strengths of $L1_2\text{Co}_3(\text{Al}, \text{W})$ in comparison with Ni_3Al are investigated using the first-principles method. Results for the stress-strain relationships, ideal tensile and shear strengths are presented. The calculated elastic properties agree well with the experimental observations. $\text{Co}_3(\text{Al}, \text{W})$ is found to have larger moduli and higher strengths, but less ductile than Ni_3Al . The electronic structures indicate the directional covalentlike Co–W bonding through d - d hybridization is the origin of excellent mechanical properties of $\text{Co}_3(\text{Al}, \text{W})$. © 2009 American Institute of Physics. [DOI: 10.1063/1.3170752]

During the past decades, Ni-base superalloys are the most widely used conventional structural materials in turbine blades for power generation and aircraft engines due to their superior mechanical properties at elevated temperature.¹ Until recently, the discovery of a Co-base alloy showing excellent high temperature strengths provides a pathway to develop more advanced superalloys.² The morphology of the Co-base alloys is identical to the microstructure of Ni-base superalloys, which is the ordered $L1_2\gamma'$ - $\text{Co}_3(\text{Al}, \text{W})$ phase coherently embedded in the disordered γ -Co solid-solution matrix. By stabilizing of the γ' phase via higher-order alloying elements, the high-temperature strength of Co-base superalloys can be improved and has a potential for high-temperature structural applications.^{3,4} Generally speaking, it is the γ' phase which is largely responsible for the strength of the superalloys. Therefore, a study of the mechanical behaviors of the $L1_2\text{Co}_3(\text{Al}, \text{W})$ and Ni_3Al would partially reflect the global properties of their alloys. So far, the mechanical properties of $L1_2\text{Co}_3(\text{Al}, \text{W})$ have been studied by both first-principles calculations and experiments.^{5–7} The elastic moduli combined with the stress-strain relationships would provide a comprehensive understanding of the mechanical properties of $\text{Co}_3(\text{Al}, \text{W})$.

The ideal strength of a material dominated by atomic bonding is the minimum stress required to yield or break a perfect crystal. It has been accepted as an essential mechanical parameter of materials. Recently, first-principles methods have been used to calculate the ideal strength of materials.^{8,9} The intrinsic strengths of many metals and intermetallic compounds have been studied.¹⁰ However, there is no study of ideal strength of $\text{Co}_3(\text{Al}, \text{W})$ reported in the literature. The present paper deals with a first-principles investigation on the mechanical properties of $L1_2\text{Co}_3(\text{Al}, \text{W})$ in comparison of Ni_3Al . Combined with the elastic moduli, the ideal strengths would provide further understanding of the mechanical properties of Co-base and Ni-base superalloys.

The first-principles calculations presented here have been carried out using the VASP code.¹¹ The generalized gradient approximation of projector augmented wave method¹²

is adopted for parametrization of the exchange-correlation functional. The plane wave cutoff energy is 300 eV. The k -point is generated in a regular Monkhorst–Pack scheme. Relaxation is done until the force is less than 0.01 eV/Å. The effect of spin polarization has been considered for the ferromagnetic nature of Co and Ni. The elastic properties are evaluated by means of the total energies calculated as function of suitable applied strains.¹³ To determine the ideal strength, we adopt the standard approach as described in Refs. 8 and 9. The stress-strain curves are simulated by incrementally deforming the unit cell in the imposed strain direction. The atomic basis vectors perpendicular to the applied strain are simultaneously relaxed until the other stress components vanish. Meanwhile, all the internal freedoms of the atom are relaxed at each step. The starting atomic positions at each step are taken from the previous step, which ensures the stress-strain curves are continuous. The nominal composition for the $\text{Co}_3(\text{Al}, \text{W})$ supercell in our calculation is Co 12.5 at. % Al 12.5 at. % W.

Table I lists the calculated lattice parameter a_0 and elastic properties of both $\text{Co}_3(\text{Al}, \text{W})$ and Ni_3Al , the corresponding results from experiments and previous calculations are

TABLE I. The calculated elastic properties of $L1_2\text{Co}_3(\text{Al}, \text{W})$ and Ni_3Al , the experimental results and other calculations are also listed for comparison.

	$\text{Co}_3(\text{Al}, \text{W})$			Ni_3Al	
	Previous work	Expt.	Others ^a	Previous work	Expt.
a_0 (Å)	3.565	3.599 ^b	3.571	3.568	3.57 ^c
B (GPa)	213.3	205 ^d	247.7	174.9	174.3 ^e
c_{11} (GPa)	301.2	271 ^d	363.4	229.7	227 ^e
c_{12} (GPa)	169.4	172 ^d	190.0	147.5	148 ^e
c_{44} (GPa)	172.1	162 ^d	211.6	116.6	120 ^e
G_h (GPa)	117.1	101 ^d	148.0	76.8	77.0 ^e
E_h (GPa)	297.0	260 ^d	370.3	201	201 ^e
G_h/B	0.549	0.493 ^d	0.60	0.44	0.44 ^e
ν	0.268	0.289 ^d	0.251	0.308	0.308 ^e

^aReference 5.

^bReference 2.

^cReference 15.

^dReference 6.

^eReference 16.

^{a)}Author to whom correspondence should be addressed. Electronic mail: wangyunjiang05@mails.tsinghua.edu.cn.

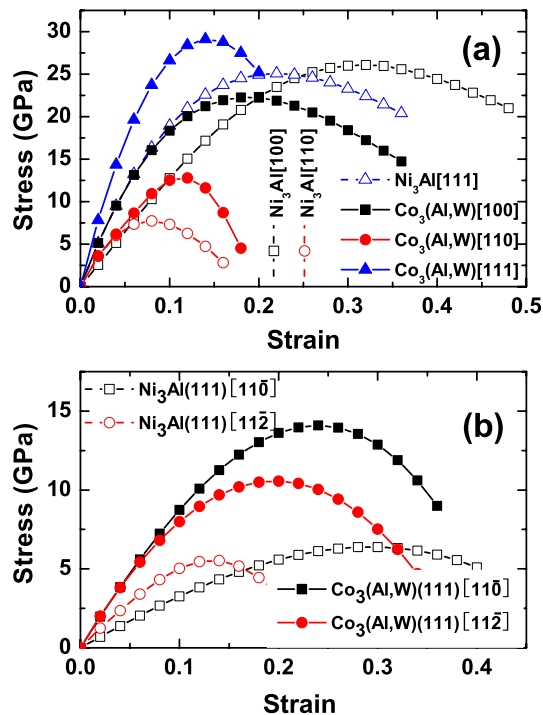


FIG. 1. (Color online) The stress-strain relationships for $\text{Co}_3(\text{Al,W})$ and Ni_3Al under (a) tension and (b) shear.

also listed. The shear and Young's moduli are estimated from the Hill's averaging method.¹⁴ Our calculated lattice parameter of $\text{L}_{12}\text{Co}_3(\text{Al,W})$ is 3.564 Å, which agrees well with the experimental values of 3.599 Å and previous calculated result of 3.571 Å. Our calculated elastic constants and moduli are in better agreement with the experimental results than previous calculations. The overestimate of the moduli in our calculations compared with the experimental values from Tanaka *et al.*⁶ attributes to the different composition of $\text{Co}_3(\text{Al,W})$, which is Co 10 at. % Al 11 at. % W for the experiment. More W–Co bonding in our model leads to higher moduli. Moreover, the corresponding calculated results for Ni_3Al are nearly identical to the experimental observations. In contrast with Ni_3Al , $\text{Co}_3(\text{Al,W})$ has larger modulus, which indicates its excellent intrinsic mechanical properties and the potential interest of applications. Furthermore, the G/B ratio of $\text{Co}_3(\text{Al,W})$ is slightly larger than that of Ni_3Al , implying the former compound is more brittle in nature according to Pugh's empirical rule.¹⁷ The result can also be concluded from the smaller Poisson's ratio of $\text{Co}_3(\text{Al,W})$. Nevertheless, $\text{Co}_3(\text{Al,W})$ should still be regarded as a ductile material since the G/B value of 0.549 is still below 0.57, which is commonly regarded as a value to separate the ductile and brittle material.¹⁷ This conclusion is in contrast with the previous calculation from Yao *et al.*⁵ but consistent with the experiment from Tanaka *et al.*⁶ and Miura *et al.*⁷ The ductile nature of $\text{Co}_3(\text{Al,W})$ enables it to be practically used as the γ' -phase of Co-base superalloys.

The stress-strain relationships for both $\text{L}_{12}\text{Co}_3(\text{Al,W})$ and Ni_3Al under tensile and shear are shown in Figs. 1(a) and 1(b), respectively. It can be seen from Fig. 1(a) that the ideal tensile strength in the [110] direction is the lowest, suggesting [110] is the easiest tensile direction for both $\text{Co}_3(\text{Al,W})$ and Ni_3Al . As shown in Fig. 1(a), [111] is the hardest tensile direction of $\text{Co}_3(\text{Al,W})$, which is different

from Ni_3Al , whose tensile strengths along [100] and [111] directions are similar. In detail, the calculated tensile strength of $\text{Co}_3(\text{Al,W})$ in [100], [110], and [111] directions are 22.3, 12.8, and 29.1 GPa, respectively. In contrast, the corresponding values for Ni_3Al are 26.1, 7.7, and 25.1 GPa, respectively. For the [110] and [111] tension, the ideal strengths of $\text{Co}_3(\text{Al,W})$ are considerably larger than that of Ni_3Al . Interestingly, [100] tensile direction behaves differently. The reason is that the directional Co–W bonding lies mainly through the [110] crystal direction, which can be seen in the charge density difference of $\text{Co}_3(\text{Al,W})$. It should be pointed out that the tensile strength from our calculation is much higher than that from the experiment.⁷ The reason is that the ideal strength derived in our paper is the maximum values of defect-free material. It sets an upper limit of the strength of a real material. On the other hand, the critical tensile strains in [100], [110], and [111] directions for $\text{Co}_3(\text{Al,W})$ are found to be 0.18, 0.12, and 0.14. Compared with 0.32, 0.08, and 0.22 for Ni_3Al , $\text{Co}_3(\text{Al,W})$ yields at smaller strains. This is consistent with the conclusion that $\text{Co}_3(\text{Al,W})$ is more brittle than Ni_3Al .

It can be observed from Fig. 1(b) that the ideal shear strength of (111)[$\bar{1}10$] direction is larger than that of (111) \times [$\bar{1}1\bar{2}$] for both two intermetallics. The result is consistent with the experimental observations that (111) \langle 112 \rangle shearing is the dominant deformation mode of $\text{Co}_3(\text{Al,W})$.³ The ideal shear strengths for $\text{Co}_3(\text{Al,W})$ in the (111)[$\bar{1}10$], and (111) \times [$\bar{1}1\bar{2}$] slip directions are 14.1 and 10.6 GPa, respectively, which is much larger than the corresponding values of 6.4 and 5.5 GPa for Ni_3Al . Such higher ideal shear strength of $\text{Co}_3(\text{Al,W})$ than Ni_3Al may indicate a bright applicable prospect of the Co-base superalloys. It is also noticed that the critical shear strain for $\text{Co}_3(\text{Al,W})$ in the (111)[$\bar{1}10$] slip directions is 0.24, which is smaller than the corresponding values of 0.30 for Ni_3Al . This is due to the partly covalent Co–W bonding along the [110] direction, which is harder than the metallic Ni–Al bonding in Ni_3Al . On the other hand, the critical shear strains for the two materials in the (111) \times [$\bar{1}1\bar{2}$] direction are close to each other, because the Co–W bond affects little on the strain in [112] direction.

In order to obtain a deeper sight into the origin of excellent mechanical properties of $\text{Co}_3(\text{Al,W})$, the partial density of states (p-DOS) are provided, as shown in Fig. 2. The results for Ni_3Al are also plotted for comparison. As shown in Fig. 2(a), a deep valley near the Fermi level called “pseudogap” separates the bonding and antibonding regions of Co-*d* and W-*d* orbitals. This feature of p-DOSs indicates there is strong interaction between Co and W atoms through *d-d* hybridization, which can be seen from the resonant hybridization peaks noted by the dotted lines in Fig. 2(a). The pseudogap in the p-DOSs also indicates the existence of directional covalentlike bonding in Co–Al–W system. The directional bonding can effectively resist the elastic and plastic deformations and results in high elastic moduli and ideal strengths. This finding also answers the question why $\text{Co}_3(\text{Al,W})$ have high G/B values and more brittle than Ni_3Al . Moreover, there also exists hybridization between Al-*p* and W-*d*, Co-*d* orbitals in the Co–Al–W system, which contributes to the mechanical properties as well. In addition, Fig. 2(b) shows the Ni-*d* and Al-*p* orbitals in Ni_3Al system. Less

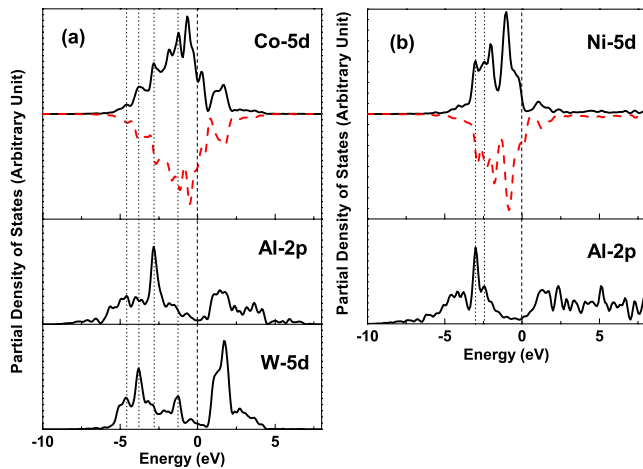


FIG. 2. (Color online) The p-DOSs for (a) Co, Al, and W atoms in $\text{Co}_3(\text{Al}, \text{W})$ and (b) Ni and Al atoms in Ni_3Al . The dashed and dotted lines imply the Fermi level and the locations of the hybridization peaks, respectively.

d-p orbital hybridization peaks indicate the bonding in Ni_3Al are weaker than that of $\text{Co}_3(\text{Al}, \text{W})$.

Besides p-DOSs, the charge density difference on the (100) planes of $\text{Co}_3(\text{Al}, \text{W})$ and Ni_3Al are plotted in Figs. 3(a) and 3(b) to understand the bonding nature. From Fig.

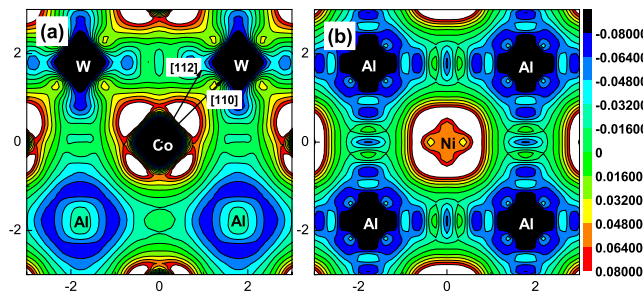


FIG. 3. (Color online) The charge density difference on (100) planes of (a) $\text{Co}_3(\text{Al}, \text{W})$ and (b) Ni_3Al . Positive (negative) values denote charge accumulation (depletion) [in unit of $e(\text{a.u.})^{-3}$].

3(a) we can see that strong charge correction regions appear around Co and W atoms, especially along the [110] crystal directions. This again confirms the existing of directional covalentlike bonding between Co and W. This bonding feature should considerably enhance the ideal tensile strength of $\text{Co}_3(\text{Al}, \text{W})$ along the [110] and [111] directions, while the effect on [100] is slight. Besides tension, the partly covalent bonding influences a lot on the shear strengths. Compared with $\text{Co}_3(\text{Al}, \text{W})$, the bonding in Ni_3Al takes on an obvious metallic bonding characteristic, which correlates much to the malleability and ductility. Furthermore, the Ni–Ni bonding along the [100] direction leads to a high tensile strength. In a word, the charge redistribution provides us with a clear picture of electronic structure origin why $\text{Co}_3(\text{Al}, \text{W})$ has higher strengths and moduli, and more brittle than Ni_3Al .

A financial grant of the “973 Project” (Ministry of Science and Technology of China, Grant No. 2006CB605102) is gratefully acknowledged.

- ¹T. M. Pollock and S. Tin, *J. Propul. Power* **22**, 361 (2006).
- ²J. Sato, T. Omori, K. Oikawa, I. Ohnuma, R. Kainuma, and K. Ishida, *Science* **312**, 90 (2006).
- ³A. Suzuki, G. C. DeNolf, and T. M. Pollock, *Scr. Mater.* **56**, 385 (2007).
- ⁴A. Suzuki and T. M. Pollock, *Acta Mater.* **56**, 1288 (2008).
- ⁵Q. Yao, H. Xing, and J. Sun, *Appl. Phys. Lett.* **89**, 161906 (2006).
- ⁶K. Tanaka, T. Ohashi, K. Kishida, and H. Inui, *Appl. Phys. Lett.* **91**, 181907 (2007).
- ⁷S. Miura, K. Ohkubo, and T. Mohri, *Mater. Trans.* **48**, 2403 (2007).
- ⁸D. Roundy, C. R. Krenn, M. L. Cohen, and J. W. Morris, *Phys. Rev. Lett.* **82**, 2713 (1999).
- ⁹D. Roundy, C. R. Krenn, M. L. Cohen, and J. W. Morris, *Philos. Mag. A* **81**, 1725 (2001).
- ¹⁰S. Ogata, Y. Umeno, and M. Kohyama, *Modell. Simul. Mater. Sci. Eng.* **17**, 013001 (2009).
- ¹¹G. Kresse and J. Hafner, *Phys. Rev. B* **48**, 13115 (1993).
- ¹²G. Kresse and J. Joubert, *Phys. Rev. B* **59**, 1758 (1999).
- ¹³S. Q. Wang and H. Q. Ye, *J. Phys.: Condens. Matter* **15**, 5307 (2003).
- ¹⁴R. Hill, *Proc. Phys. Soc., London, Sect. A* **65**, 349 (1952).
- ¹⁵M. H. Yoo, *Acta Metall.* **35**, 1559 (1987).
- ¹⁶M. J. Mehl, B. M. Klein, and D. A. Papaconstantopoulos, in *Intermetallic Compounds: Principles and Practice*, edited by J. H. Westbrook and R. L. Fleisher (Wiley, New York, 1994), Vol. 1, pp. 195–209.
- ¹⁷S. F. Pugh, *Philos. Mag.* **45**, 823 (1954).